



Research paper

A theoretical investigation of sugar and phosphate contributions to the activation barriers of guanine methylation by carcinogenic methane diazonium ion

Arturo Rojas, Samantha Cabal, George A. Papadantonakis*

Department of Chemistry, University of Illinois at Chicago, 845 W. Taylor St., Room 4500 SES, Chicago, IL 60607, United States

HIGHLIGHTS

- Methylation of guanine at N7.
- CPCM and discrete/SCRF solvation models.
- Carcinogenic methane diazonium ion and S_N2 mechanism.
- Electrostatic potential and local ionization maps.
- Activation barriers.

A B S T R A C T

Feedback from electrostatic potential and local ionization potential maps provides evidence that in the gas phase electrostatic interactions cause the activation barriers of guanine methylation by methane diazonium ion at the N7 site to increase upon addition of sugar and phosphate moieties, from 24.6 kcal/mol with the 6–31 + G* basis set to 29.87 kcal/mol with the 6–311 + G (2df, 2p) basis set at the DFT/B3LYP-D3 level of theory. Aqueous activation barriers strongly depend on the interaction of guanine with discrete number of water molecules and, in implicit water, they lie between 4.37 for free guanine to 5.39 kcal/mol for *syn*-dGMP[−]

1. Introduction

Guanine methylation is directly related to mutagenic and carcinogenic activity and the N7 and O^6 are the predominant sites to be methylated [1–3]. Most *N*-nitroso compounds have carcinogenicity due to alkylation of DNA bases by alkane diazonium ions, such as methane diazonium ion, $CH_3N_2^+$ [4]. The methane diazonium ion is the reactive intermediate formed from direct acting methylating agents such as, *N*-methyl-*N*-nitrosourea (MeNU) [3], *N*-methyl-*N'*-nitro-*N*-nitrosoguanidine (MNNG) [5], triamethyltriazenes [6], methylnitrosocarbamates and nitrosamines [4]. The methane diazonium ion is actually an electrophile cation and has great ability to undergo sequence specific reactions with guanine at the N7 and O^6 nucleophilic sites [7–9]. Temozolamide is a widely used chemotherapeutic agent in brain tumors, and it is also known to methylate DNA via methane diazonium ions that are formed as intermediates [10]. It is well established that the N7 position of guanine is the most vulnerable site for methylation [1], and that guanine is the most easily damaged among the four DNA bases by ionizing radiation in aqueous solutions [11,12].

The methylation of DNA bases by $CH_3N_2^+$ occurs through a bimolecular S_N2 nucleophilic substitution mechanism [3,13,14] and the experimental selectivity observed at different sites indicate the existence of an activation barrier [1,15]. In a theoretical investigation of the effect of sugar moiety on the reactivity of methane diazonium ion towards the N7 site of guanine, it is reported that reactivity increases in the order of guanine > 2'-deoxyguanosine > guanosine and therefore, the addition of sugar moiety to guanine causes its reactivity to decrease [16]. In the same study it is also reported that the activation energies of the methylation reactions are basis set dependent and they are increased by ~12% at the B3LYP level as the basis set becomes larger, from 6–31G (d, p) to aug-cc-pVDZ and that the values determined at the B3LYP/ aug-cc-pVDZ//B3LYP/6-31G (d, p) change by ~1–4% versus those determined at the B3LYP/ aug-cc-pVDZ level.

In another theoretical investigation, it was reported that the ordering of activation energies and partial bond distances at the transition states obtained by DFT/B3LYP/6–31 + G* and MP2/6–31 + G* levels of theory are similar, but the latter calculation is 30 times more computational expensive [17]. In the same investigation it was also

* Corresponding author.

E-mail address: gpapad3@uic.edu (G.A. Papadantonakis).

<https://doi.org/10.1016/j.cplett.2018.10.063>

Received 31 August 2018; Received in revised form 22 October 2018; Accepted 23 October 2018

Available online 29 October 2018

0009-2614/ © 2018 Published by Elsevier B.V.

reported that the combined discrete/SCRF hydration energy calculations using base-water complexes with three water molecules yield base hydration energies that are larger than those obtained from the conductor-like polarizable continuum model (CPCM) [17]. In another theoretical investigation it was reported that the methylation of DNA bases by CH_3N_2^+ employing the B3LYP/6-31G** and MP2/6-31G** levels of theory yield, in the gas phase, have relatively small activation energy (< 8.01 kcal/mol), and that the methylation process is exothermic and easy to occur [18].

Theoretical calculation results employing the DFT/M06-2X/6-31 + G*/CPCM and DFT/B3LYP-D3/6-311 + G (2df, 2p) levels of theory and feedback from electrostatic potential maps show that, in water, charge separation between the nucleic acid base and the leaving group results in reduced hydrogen bond interactions and the activation energy for the $\text{S}_{\text{N}}2$ methylation reactions by dimethyl sulfate is lowered, compared to the gas-phase, at all N sites of the bases considered in the study except for the O^6 site in guanine [19]. Consequently, the percent methylation in water increases as the activation barriers decrease [1].

It is established that for DNA bases, alkylation increases as the first π ionization potential of the nucleotide base decreases [15], and that guanine has the lowest ionization potential among DNA bases [12,20]. In another theoretical investigation, employing the DFT/B3LYP/6-31 + G*/SM8 level of theory, it was reported that the aqueous photoionization energy of guanine, (G), is 4.68 eV, *anti*-2'-deoxyguanosine, (*anti*-dG), is 4.78 eV, and *syn*-2'-deoxyguanosine 5'-monophosphate, (*syn*-dGMP⁻), is 4.61 eV [21].

The impact of the N7-methylguanine, (N7mG), on mutagenesis is under question. On one hand, there is an argument that the N7mG does not affect the Watson-Crick base pairs during DNA replication and, therefore, it is not considered as a potent mutagen but the O^6 -methylguanine, (O^6 mG), is known for its mutagenicity. The O^6 mG changes the hydrogen bond properties of guanine because of deprotonation at the N1 site of guanine that can result to the inhibition of the Crick-Watson base pair configuration and to further mispairing by DNA polymerase [22]. The buildup of O^6 mG can lead to its misreading as an adenine base pairing to a thymine base and this initiates DNA mutations [23–27]. On the other hand, in a crystallographic study, it was reported that the N7 methylation alters the hydrogen-bonding patterns of guanine in duplex DNA and, although N7mdG leaves unmodified the Watson-Crick base-pair region, it can affect the base-pairing properties of guanine via electronic and steric effects inducing mutagenesis [28].

In light of the aforementioned contradicting reports the focus of the work in this investigation is to further examine factors that influence the activation barriers for reactions of methane diazonium ion with free base G, *anti*-dG, and *syn*-dGMP⁻ at the N7 site of guanine in the gas phase and in water.

2. Methods

All calculations were performed using the Spartan '16 Parallel Suite [29] for Microsoft Windows 7, Professional 64-bit edition on an Intel Xeon E3-1240 v3 processor utilizing 32 GB of RAM. Standard geometries of the molecules investigated were generated using the Molecule Builder of Spartan '16 and were fully optimized employing the Density Functional Theory (DFT) using the dispersion-corrected density functional B3LYP-D3 with the 6-31 + G* and 6-311 + G (2df, 2p) basis

Table 1

Gas-phase transition state geometries and activation energies corrected for the zero-point-energy calculated at the DFT/B3LYP-D3/6-311 + G (2df, 2p) level of theory.

Molecule	r_{forming} (Å)	r_{breaking} (Å)	E_a (kcal/mol)	Distortion Angle (deg)	E_a (ZPE) (corr) (kcal/mol)	Im. freq. (cm^{-1})
<i>syn</i> -N7mdGMP ⁻	1.906	1.321	35.96	69.58	37.32	-189
<i>anti</i> -N7mdG	2.013	1.310	35.26	68.13	36.24	-130
N7mG	2.438	1.397	11.39	62.52	7.45	-138

sets. The zero-point energy, (ZPE), corrections for the gas-phase activation barriers are also used.

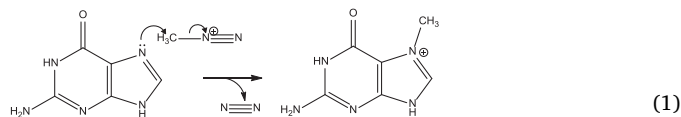
The $\text{S}_{\text{N}}2$ transition states of the methylation reactions were monitored by employing the Energy Profile module in Spartan '16. The optimized structures were confirmed to be true transition states by calculating the normal modes and finding one and only one imaginary frequency [30].

Both the 6-31 + G* and the 6-311 + G (2df, 2p) basis sets include polarization functions on all atoms and diffuse functions on heavy atoms and the later basis set includes more of such functions than the former. Diffuse functions on heavy atoms are important for this project because the bases have lone pairs and polarization functions on all atoms, which affects the geometry and the energetics of the reaction profiles. Therefore, the basis sets selected constitute an appropriate treatment for the present study.

Solvation energy calculations were performed by employing the conductor-like polarizable continuum model (CPCM) with water being the implicit solvent with dielectric constant of 78.3 [31–33].

3. Results and discussion

The reaction mechanism of guanine with methane diazonium ion, CH_3N_2^+ , is an $\text{S}_{\text{N}}2$ reaction characterized by the fact that guanine, the dinitrogen leaving group (N_2) and the carbon atom of methane diazonium ion are approximately linear. In a typical $\text{S}_{\text{N}}2$ reaction the attack angle must be at 180° because this angle provides the maximum overlap between the lone pair of electrons on N7 of guanine and the σ^* antibonding orbital of C–X, (X = leaving group). The leaving group is then pushed off the opposite side and the product is formed in the reaction under consideration the leaving group is dinitrogen, which is a very good leaving group [34]. The $\text{S}_{\text{N}}2$ reaction mechanism is shown below in Eq. (1).



In fact the angle, in implicit water calculations, between the N7 atom of free guanine, the C atom of methane diazonium and the N atom of the dinitrogen leaving group is 173.3° , but in the gas phase the distortion of the attack angle from linearity is significant, 62.52° , as listed in Table 1.

Table 1 contains gas-phase transition state geometries and activation energies for the methylation of guanine at the N7 site corrected for the zero-point-energy (ZPE). It contains also the distances for forming and breaking bonds calculated at the DFT/B3LYP-D3/6-311 + G (2df, 2p) level of theory. The imaginary frequencies of the transition states in the gas-phase are also reported and they correspond to the normal mode of vibration of the bond formed by the reaction center N7 and the carbon of the methyl group in CH_3N_2^+ , and the breaking bond between the carbon of the methyl group and the nitrogen of the leaving group. In addition, results in Table 1 indicate that the forming bond distances in the transition states for the reactions at the N7 atom become shorter as the sugar and phosphate moieties are added. These distances range from 1.906 Å for the N7 methylation of *syn*-dGMP⁻, to 2.013 Å for the *anti*-dG, and to 2.438 Å for the free guanine base.

Fig. 1 shows the gas-phase transition state geometries at the N7

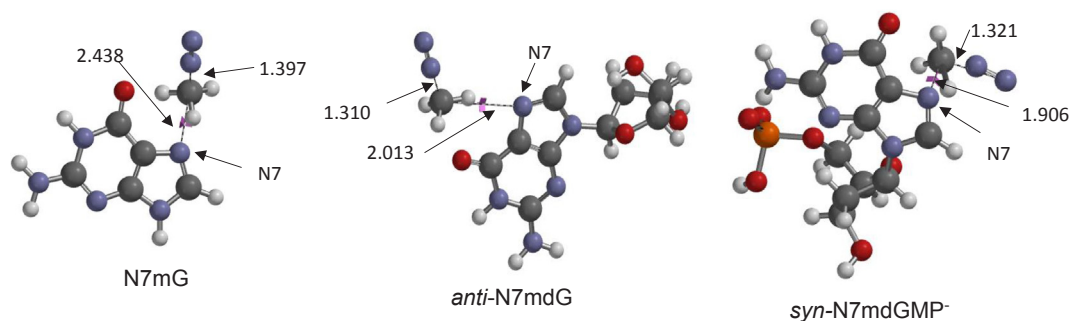


Fig. 1. Gas-phase transition state structures optimized at the DFT/B3LYP-D3/6–311 + G (2df, 2p) level of theory of (a) N7m G, (b) *anti*-N7mdG, and (c) *syn*-N7mdGMP⁻. The forming bond distance in (a) between N7 and C of the methane diazonium ion is 2.438 Å and the breaking bond distance of the leaving group (N₂) between the C atom of methane diazonium ion and nitrogen is 1.397 Å. The same distances in (b) are 2.013 Å and 1.310 Å and in (c) are 1.906 Å and 1.321 Å.

methylation site for all three molecules under consideration. Here, the attack angle between the lines containing the carbon atom in the methane diazonium ion and the reaction center on the base, and the plane of the base show a deviation from linearity. The values of the attack angle distortion from linearity for the methylation at the N7 site of *syn*-dGMP⁻ is 69.58° and of *anti*-dG is 68.13° and the values for the activation energy of methylation at N7 is 35.96 kcal/mol and 35.26 kcal/mol respectively. The attack angle distortion in the transition state of N7mG is 62.52° and the activation energy is 7.45 kcal/mol. These results clearly indicate that the addition of the sugar moiety in the free base significantly affects the activation energy of the methylation reaction at N7, but the addition of the phosphate moiety in the nucleoside increases the activation energy only by 1.08 kcal/mol.

It is observed that in the transition state of N7mG, the distortion of the attack angle is considerable. The employment of the electrostatic maps, in Fig. 2, may provide feedback to understand the reason for the distortion of the attack angle.

Fig. 2 (a–c) shows the gas-phase electrostatic potential maps of N7mG, *anti*-N7mdG, and *syn*-N7mdGMP⁻ respectively. The electrostatic potential maps were computed using the DFT/B3LYP-D3/6–311 + G (2df, 2p) level of theory and the electrostatic potential maps were drawn by the module embedded in Spartan '16. The electrostatic maps show the electrostatic potential on a surface of electron density. Colors near red represent large negative values of the potential and they show that charge is localized in this area, colors near blue represent large positive values and green colors represent intermediate values of the potential and that the charge is delocalized in that areas.

Fig. 2(a) shows charge delocalization around the N7 reaction center and development of negative charge in the N₂ leaving group and around O⁶. The electrostatic potential at the N₂ reaction center is -76.2 kJ/mol and at the N₂ leaving group is -145.5 kJ/mol. At the center of the imidazole ring of guanine the electrostatic potential is -21.5 kJ/mol. The distance of the forming bond between the N7 and the carbon of the methyl group of CH₃N₂⁺ is long, (2.438 Å), and the distance of the breaking bond is also long, (1.397 Å). The increased atom separation, in order to minimize the unfavorable steric interaction, leads to an increased charge-charge separation, and consequently to a decrease in electrostatic energy. The immediate consequence of this charge separation is the deviation from linearity of the transition state attack angle.

Fig. 2(b) shows the electrostatic potential map of the *anti*-N7mdG. Here, the governing color in this map is blue, which means positively charged areas with a few green areas around O⁶ and in the middle of the imidazole ring of guanine. The electrostatic potential at the N7 reaction center is 263.4 kJ/mol and at the N₂ leaving group is 498.8 kJ/mol. The distance of the forming and breaking bonds decrease compared to N7mG by 0.425 Å and 0.087 Å respectively. The addition of sugar and the release of dinitrogen contribute more to the delocalization of the positive charge in the imidazole ring of *anti*-dG and this results to the observed strong stabilization upon methylation. This conclusion is in line with the low ionization potential in water of *anti*-dG, 4.69 eV, as calculated employing the B3LYP/6–31 + G*/SM8 level of theory [21]. The experimental value of the ionization potential in water for *anti*-dG is 4.77 eV [35]. In addition, charge delocalization weakens the

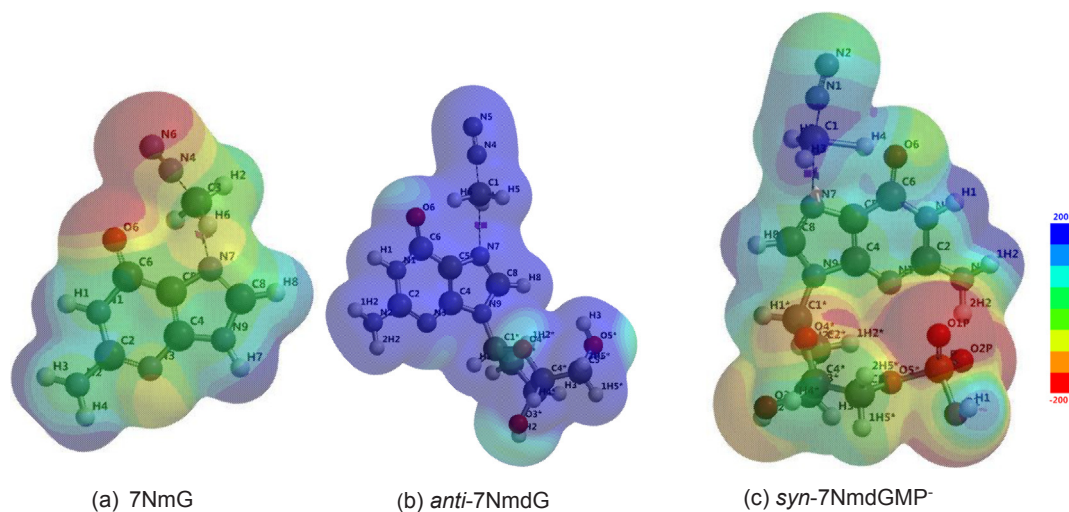


Fig. 2. Electrostatic potential maps of (a) N7mG, (b) *anti*-N7mdG, and (c) *syn*-N7mdGMP⁻. The electrostatic maps were computed using the DFT/B3LYP-D3/6–311 + G (2df, 2p) level of theory. Colors near red represent large negative values of the potential and they show that charge is localized in this area, colors near blue represent large positive values and green colors represent intermediate values of the potential and that charge is delocalized in that areas.

Table 2

Transition state geometries and activation energies calculated with implicit water at the DFT/B3LYP-D3/6–31 + G* level of theory and the CPCM Model.

Molecule	E_a (aq) (kcal/mol)	Attack Angle (deg)	r_{forming} (Å)	r_{breaking} (Å)
<i>syn</i> -N7mdGMP [−] (implicit)	5.34	177.19	2.331	1.576
<i>anti</i> N7mdG (implicit)	5.18	175.96	2.119	1.613
N7mG (implicit)	4.37	173.03	2.367	1.557

N-glycosidic bond and the latter can break at a rate several orders of magnitude greater than that of the unsubstituted purines [36].

In Fig. 2(c), the electrostatic potential map of *syn*-N7dGMP[−] shows that there is charge separation between the N7 reaction center and the N₂ leaving group. The electrostatic potential at N7 is slightly positive at 33.8 kJ/mol, at the N₂ leaving group is 148.1 kJ/mol, and at the center of the imidazole ring is 15.2 kJ/mol. Here, the electrostatic potential value of the sugar is negative, −102.1 kJ/mol, and of the phosphate is −242.10 kJ/mol. This charge separation in the nucleotide components is in line with the low ionization potential of *syn*-dGMP[−], 4.61 eV [21]. The forming bond distance in *syn*-N7dGMP[−] is shorter (1.906 Å) than in N7mG and *anti*-N7mdG. The gas-phase activation barrier values in both *anti*-N7mdG and *syn*-N7mdGMP[−] are very close in value, 36.24 kcal/mol and 37.32 kcal/mol respectively.

Table 2 lists the aqueous activation energies for the transition states at the N7 site of guanine for all three molecules under consideration. The activation energies, in implicit water, are calculated at the DFT/B3LYP-D3/6–31 + G* level of theory employing the CPCM method. The choice of the 6–31 + G* basis set for the evaluation of the activation barriers in water was based merely on grounds of computational expense. The results obtained show that the aqueous activation energy, E_a (aq), for the methylation at the N7 site is 4.370 kcal/mol for N7mG, 5.180 kcal/mol for *anti*-N7mdG and 5.39 kcal/mol for *syn*-N7mdGMP[−]. The attack angles in the transition states, in water, are close to linearity and their values are 173.03° for N7mG, 175.96° for *anti*-N7mdG, and 177.19° for *syn*-N7mdGMP[−]. In addition the forming bond distance in N7mG is 2.367 Å and the breaking bond distance is 1.557 Å. In *syn*-N7mdGMP[−] these bond distances become 2.331 Å and 1.576 Å respectively. In *anti*-N7mdG the forming bond distance becomes shorter, (2.119 Å), than at N7mG and *syn*-N7mdGMP[−] and the breaking bond distance becomes larger, (1.613 Å). Finally, the attack angle in the transition state in *anti*-N7mdG deviates from linearity only by 4.040°. These results are in agreement with previous reported theoretical investigations employing the DFT method with B3LYP/6–31 + G* and CPCM [17] and B3LYP and M06-2X functionals with 6-31G (d, p) and aug-cc-pVDZ basis sets [16].

The linearity of the attack angle is the main characteristic of S_N2

Table 3

Gas- phase transition state geometries and activation energies calculated at the DFT/B3LYP-D3/6–31 + G* level of theory.

Molecule	r_{forming} (Å)	r_{breaking} (Å)	Attack Angle (deg)	E_a (kcal/mol)
<i>syn</i> -N7mdGMP [−]	1.906	1.390	176.86	34.15
<i>anti</i> -N7mdG	2.119	1.395	150.64	31.68
N7mG	2.508	1.404	112.44	9.54

Table 4

Transition state geometries and activation energies calculated with discrete molecules of water at the DFT/B3LYP-D3/6–31 + G* level of theory and the CPCM Model.

Molecule	E_a (aq) (kcal/ mol)	Attack Angle (deg)	r_{forming} (Å)	r_{breaking} (Å)
<i>syn</i> -N7mdGMP [−] + 1 H ₂ O	6.33	177.02	2.331	1.584
<i>syn</i> -N7mdGMP [−] + 3 H ₂ O	7.92	177.66	2.331	1.580
<i>anti</i> -N7mdG + 1 H ₂ O	8.50	177.93	2.331	1.616
<i>anti</i> -N7mdG + 3 H ₂ O	7.83	176.08	2.331	1.564
N7mG + 1 H ₂ O	7.54	123.27	2.579	1.421
N7mG + 3 H ₂ O (a) [*]	6.42	177.74	2.367	1.528
N7mG + 3 H ₂ O (b) [*]	62.16	84.80	1.871	1.476

* Structures (a) and (b).

reactions. And this explains the dramatic decrease of the activation energy in implicit water, 5.39 kcal/mol, compared to the gas phase, 37.32 kcal/mol. For *anti*-N7mdG the activation barrier lowers from 36.24 kcal/mol in the gas phase to 5.18 kcal/mol in implicit water and of N7mG from 7.45 kcal/mol to 4.37 kcal/mol, respectively. The values of the aqueous activation energies are very close to each other following the order *syn*-dGMP[−] > *anti*-dG > G. Results clearly indicate that, in implicit water, the addition of the sugar and phosphate moieties to the free base affect the activation energy of the methylation of guanine at the N7 site only by 1.02 kcal/mol.

Fig. 3(a) shows the electrostatic potential map for N7mG generated at B3LYP-D3/6–31 + G* but it does not reveal charge separation, as it does when the larger basis set was used and it is shown in Fig. 2(a). The electrostatic potentials on molecular surfaces can be complemented by the local ionization potential maps when processes involve charge transfer and bond formation, as is the case in electrophilic attacks [37]. Interactions with an electrophile is promoted by the combination of a strongly negative potential to initiate a strong attraction followed by a low energetic requirement for the subsequent charge transfer [38]. The local ionization potential map for N7mG is calculated at the B3LYP-D3/6–31 + G* level of theory and it is shown in Fig. 3(b), and the local ionization potential map of free guanine is shown in Fig. 3(c). It is

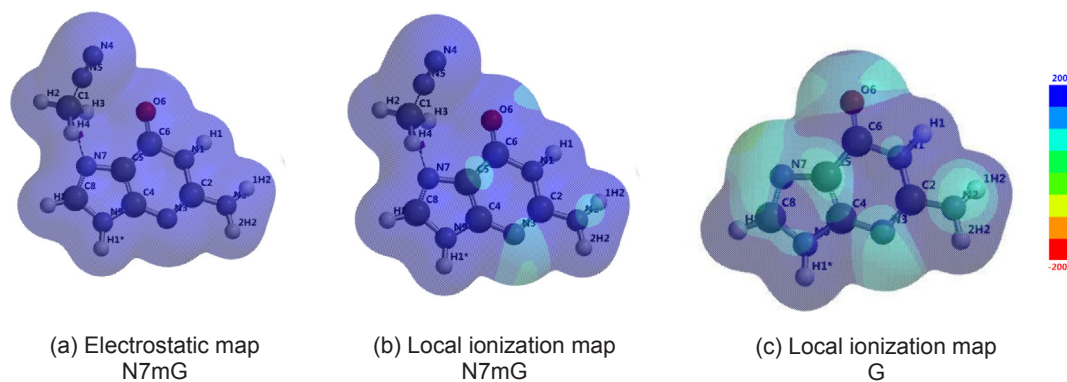


Fig. 3. Electrostatic potential map of (a) N7mG, local ionization map of (b) N7mG, and local ionization map of G calculated by the DFT/B3LYP-D3/6–31 + G* level of theory. Colors near red represent large negative values of the potential and they show that charge is localized in this area, colors near blue represent large positive values and green colors represent intermediate values of the potential and that charge is delocalized in that areas.

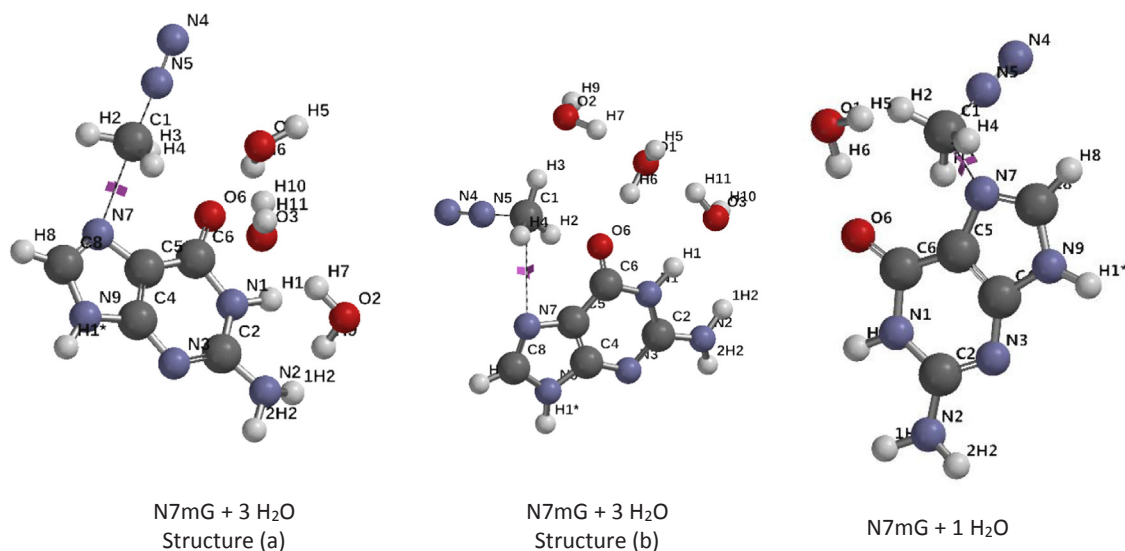


Fig. 4. Aqueous transition state structures optimized at the DFT/B3LYP-D3/6–31 + G^* level of theory and the CPCM model of (a) N7m G + 3 H_2O molecules, (b) N7m G + 3 H_2O molecules, and (c) N7m G + 1 H_2O molecule. The forming bond distance in (a) between N7 and C of the methane diazonium ion is 2.331 Å and the breaking bond distance of the leaving group (N_2) between the C atom of methane diazonium ion and nitrogen is 1.528 Å. The same distances in (b) are 1.871 Å and 1.421 Å and in (c) are 2.579 Å and 1.421 Å.

reported that the local ionization potential of guanine at the N7 site is 8.42 eV [21]. The local ionization map, in Fig. 3(b), shows that there is more electron density at N7, necessary to initiate the strong attraction followed by the delocalization of electron density. The electrophile, $CH_3N_2^+$, is not bulky and, therefore, its contribution to steric effects is not under consideration. The local ionization potential maps suggest that the deviation from linearity of the transition state attack angle and the high values of the gas-phase activation barriers can be attributed to charge separation.

Table 3 lists the methylation gas-phase transition state geometries and activation energies at the N7 reaction center of guanine, as calculated using the DFT/B3LYP-D3/6–31 + G^* level of theory. As it is indicated, in the gas-phase, the values of the transition-state attack angles are strongly basis set dependent. The use of the smaller basis set, 6–31 + G^* , yields transition-state attack angle value of 176.86° for *syn*-N7mdGMP[−], 150.64° for *anti*-N7mdG and 112.44° for N7mG.

In reaction field, SCRF, calculations the implicit water molecules are replaced by a homogeneously polarizable dielectric medium [39] and only a small number of parameters, such as cavitation, dispersion, exchange repulsion, and changes in solvent structure are used to represent the solvent with reasonable accuracy [40,41] and solvents are thermally averaged and considered to be isotropic [42]. An immediate issue with the implicit water calculations is that the dielectric continuum is not connected well to the molecule being studied and the coupling between the two is not adequately addressed. The latter can be improved with calculations involved a discrete number of water molecules.

Table 4 lists the transition state geometries and the activation barriers with 1 and 3 water molecules for the molecules of this study. For *anti*-dG and *syn*-dGMP[−] the attack angles deviate from linearity between 2 and 4° and the activation barriers are higher than the ones obtained by the implicit water calculations by 2.6–3.3 kcal/mol for the *anti*-N7mdG and 1.15–2.58 kcal/mol for the *syn*-dGMP[−].

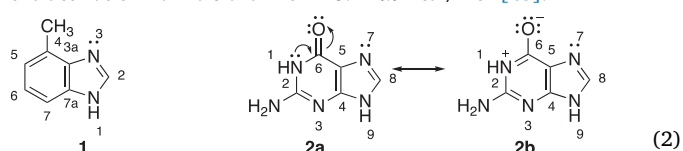
Fig. 4 shows the transition state geometry of free guanine with 3 water molecules in structures (a) and (b) and with one water molecule in structure (c). In structure (a) the attack angle is 177.74° and the activation barrier is 6.42 kcal/mol and in structure (b) the attack angle is 84.80°, a 95.2° deviation from linearity and the activation energy is 62.16 kcal/mol. In structure (c) the attack angle is 123.27°, a 56.73° deviation from linearity and the activation energy is 7.54 kcal/mol. It is noticeable that the forming bond distance in structure (b) is 1.871 Å,

which is 0.496 Å shorter than in structure (a) (2.367 Å). The forming and breaking bond distances in structure (b) show that the intramolecular hydrogen bond of the complex in the transition state leads to a tighter transition state. In structure (a) the hydrogen bond is weaker, the complex is less tight and the activation energy is considerably smaller.

Considering the geometry of water molecules, in structure (b), it is evident that the deviation of the attack angle from linearity implies strong steric effects between the water molecules and the methane diazonium ion. These steric effects result from repulsive forces between overlapping electron clouds of neighboring atoms and they cause an increase of the activation energy of the reaction.

The values for the activation barrier of the N7 methylation reaction, in implicit water, for N7mG, *anti*-N7mdG and *syn*-N7mdGMP[−] range from 4.370 to 5.390 kcal/mol. These values are in agreement with results reported in a theoretical investigation employing QM/MM-MD simulations in which the barrier for the attack of the primary diazonium ion onto a guanine embedded in a solvated dodecamer, via the PCM model, is not higher than 6.0 kcal/mol and that the Watson-Crick pairing remains unaffected upon the approach of $CH_3N_2^+$ [26].

The activation barrier values in implicit water are also in agreement with the results reported in an experimental study on the alkylation of 2-substituted-4-methylbenzimidazoles. In this study, it was reported that the electrostatic and non-bonded steric interactions are governed by the variable geometries of the S_N2 transition states involved and in particular the $N\cdots C$ distance of the developing N -alkyl bond and that the activation barriers are within 3.2–4.7 kcal/mol [43].



Benzimidazole (1) and guanine (2a), as shown in Eq. (2), have great similarity in structure and reactivity. One of the most common characteristics is their aromaticity. Both compounds are aromatic (planar), have a conjugate system of 10 π -electrons delocalized between 2 rings where a pair of electrons from the protonated nitrogen atoms 1 and 9 in benzimidazole and guanine, respectively, participates in conjugation and comprise the aromatic system with remaining 8 π -electrons of the rings. The similarities in chemical reactivity between the two molecules

can serve as a guideline about the assessment of the value of the activation barriers of the reactions under this study.

The interaction of a chemical system with water is dynamic. This fact makes it unlikely that specific geometries of the hydrated complexes persist. However, the agreement between the experimentally observed high reactivity of guanine [1] and the calculated activation barriers by the discrete/SCRF method suggests that these structures or other similar to them are statistically significant and contribute to the determination of the activation barriers.

4. Conclusions

In summary the main results obtained from this investigation are the following:

1. Both in the gas phase and in water the reactivity of N7 methylated guanine decreases as sugar and phosphate moieties are added to the free base, guanine, in the order, $\text{syn-N7mdGMP}^- < \text{anti-N7mdG} < \text{N7mG}$
2. The activation energies for the methylation reactions in the gas phase are basis set dependent and the increase in value becomes larger as the basis set becomes larger, from $6-31 + G^*$ to $6-311 + G(2df, 2p)$ at the DFT/B3LYP-D3 level of theory.
3. Combination of electrostatic potential and local ionization maps provide evidence that electrostatic interactions is the reason for the decrease in reactivity of the N7 methylated guanine as sugar and phosphate moieties are added to guanine in the gas phase.
4. The current results provide evidence that the activation barriers with discrete water molecules are strongly dependent on the interaction of the reaction system with water and these values with implicit water lie under 5.4 kcal/mol.

Acknowledgements

Samantha Cabal is grateful for the financial support provided by the University of Illinois at Chicago Liberal Arts and Science Undergraduate Research Initiative (LASURI) and the Department of Chemistry. GAP acknowledges stimulating discussions with Professor Donald J. Wink and Dr. Maria Yermolina of the UIC Chemistry Department. Daniel R. Eichler assisted with the initial calculations.

References

- [1] B. Singer, D. Grunberger, *Molecular Biology of Mutagens and Carcinogens*, Plenum Press, New York, 1983.

- [2] K.S. Gates, *Chem. Res. Toxicol.* 22 (2009) 1747.
- [3] P.D. Lawley, *Chemical Carcinogenesis*, ACS Monograph 182, Washington, D.C., 1984.
- [4] W. Lijinsky, *Chemistry and biology of N-nitroso compounds*, Cambridge University Press, Cambridge, 1992, p. 55.
- [5] P.D. Lawley, C.J. Thatcher, *Biochem. J.* 116 (1970) 693.
- [6] D.H. Shieh, C.J. Michejda, *J. Am. Chem. Soc.* 103 (1981) 442.
- [7] G. Liang, L. Encell, M.G. Nelson, C. Switzer, D.E.G. Shuker, B. Gold, *J. Am. Chem. Soc.* 117 (1995) 10135.
- [8] P. Iyer, A. Srinivasan, S.K. Singh, G.P. Mascara, S. Zayitova, B. Sidone, E. Fouquierel, D. Svirar, R.W. Sobol, M.S. Bobola, J.R. Silber, B. Gold, *Chem. Res. Toxicol.* 26 (2013) 156.
- [9] R.L. Wunderman, B. Gold, *Chem. Res. Toxicol.* 1 (1988) 146.
- [10] S.S. Agarwala, *Oncologist* 5 (2000) 144.
- [11] J. Cadet, P. Vigny, *Bioorganic Photochemistry; Photochemistry and the Nucleic Acid*, John Wiley & Sons, New York, 1990.
- [12] H. Fernando, G.A. Papadantonakis, N.S. Kim, P.R. LeBreton, *PNAS* 95 (1998) 5550.
- [13] G.P. Ford, J.D. Scribner, *Chem. Res. Toxicol.* 3 (1990) 219.
- [14] N. Nakayama, S. Tanaka, O. Kikuchi, *J. Theoret. Biol.* 215 (2002) 13.
- [15] N.S. Kim, P.R. LeBreton, *J. Am. Chem. Soc.* 118 (1996) 3694.
- [16] P.M. Shukla, K. Bhattacharjee, *Int. J. Quantum Chem.* 114 (2014) 1637.
- [17] K.S. Ekanayake, P.R. LeBreton, *J. Comput. Chem.* 27 (2005) 277.
- [18] L. Li, Z. Qu, H. Wang, Z. Li, *Science in China Series B, Chemistry* 52 (2009) 26.
- [19] D.R. Eichler, G.A. Papadantonakis, *Chem. Phys. Lett.* 689 (2017) 8.
- [20] D.M. Close, *J. Phys. Chem. A* 108 (2004) 10376.
- [21] D.R. Eichler, H.A. Hamann, K.A. Harte, G.A. Papadantonakis, *Chem. Phys. Lett.* 680 (2017) 83.
- [22] E.L. Loechler, C.L. Green, J.M. Essigmann, *Proc. Nat. Acad. Sci. USA-Biol. Sci.* 81 (1984) 6271.
- [23] Y. Mishina, E.M. Duguid, C. He, *Chem. Rev.* 106 (2006) 215.
- [24] G. Boysen, B.F. Pachkowski, J. Nakamura, J.A. Swenberg, *Mutat. Res. Genet. Toxicol. Environ. Mutagen.* 678 (2009) 76.
- [25] B. Ashwood, L.A. Ortiz-Rodríguez, C.E. Crespo-Hernández, *J. Phys. Chem. Lett.* (2017) 4380.
- [26] R. Gruber, J. Aranda, A. Bellili, I. Tunon, E. Dumont, *PCCP* 19 (2017) 14695.
- [27] M. Esteller, R.-A. Risques, M. Toyota, G. Capella, V. Moreno, M.A. Peinado, S.B. Baylin, J.G. Herman, *Cancer Res.* 61 (2001) 4689.
- [28] Y. Kou, M.-C. Koag, S. Lee, *J. Am. Chem. Soc.* 137 (2015) 14067.
- [29] *Wavefunction, Spartan '16 Parallel Suite*, Irvine, CA, 2014.
- [30] S.S. Shaik, H.B. Schlegel, S. Wolfe, *Theoretical Aspects of Physical Organic Chemistry: The S_N2 Mechanism*, John Wiley, New York, 1992.
- [31] Y. Takano, K.N. Houk, *J. Chem. Theory Comput.* 1 (2005) 70.
- [32] B. Mennucci, J. Tomasi, *J. Chem. Phys.* 106 (1997) 5151.
- [33] V. Barone, M. Cossi, J. Tomasi, *J. Chem. Phys.* 107 (1997) 3210.
- [34] M.B. Smith, *March's Advanced Organic Chemistry*, John Wiley - Interscience, New York, 2007.
- [35] G.A. Papadantonakis, R. Tranter, K. Brezinsky, Y. Yang, R.B. van Breemen, P.R. LeBreton, *J. Phys. Chem. B* 106 (2002) 7704.
- [36] Z. Shabarova, A. Bogdanov, *Advanced Organic Chemistry of Nucleic Acids*, VCH Publishers, New York, 1994.
- [37] P. Politzer, J.S. Murray, M.C. Concha, *Int. J. Quantum Chem.* 88 (2002) 19.
- [38] P. Sjöberg, P. Politzer, *J. Phys. Chem.* 94 (1990) 3959.
- [39] R.E. Skyner, J.L. McDonagh, C.R. Groom, T. van Mourik, J.B.O. Mitchell, *PCCP* 17 (2015) 6174.
- [40] C.J. Cramer, D.G. Truhlar, *Acc. Chem. Res.* 41 (2008) 760.
- [41] C. Maurizio, R. Nadia, S. Giovanni, B. Vincenzo, *J. Comput. Chem.* 24 (2003) 669.
- [42] C.J. Cramer, D.G. Truhlar, *Chem. Rev.* 99 (1999) 2161.
- [43] M.R. Haque, M. Rasmussen, *Tetrahedron* 50 (1994) 5535.